BIOCHEMISTRY
including biophysical chemistry & molecular biology

Article

pubs.acs.org/biochemistry

Thermal Unfolding of Apolipoprotein A-1. Evaluation of Methods and Models

Therese Schulthess,[†] Hans-Joachim Schönfeld,[‡] and Joachim Seelig*,[†]

[†]Biozentrum, University of Basel, Klingelbergstrasse 50/70, CH-4056 Basel, Switzerland

[‡]Pharma Research & Early Development, F. Hoffmann-La Roche AG, Grenzacherstrasse 124, CH 4070 Basel, Switzerland

ABSTRACT: Human apolipoprotein A-1 (Apo A-1) was used as a model protein to compare experimental methods and theoretical models for protein unfolding. Thermal unfolding was investigated in aqueous buffer, in β-octylglucoside solution, and with phospholipid bilayer vesicles. The α-helix content of Apo A-1 increased from 50% in aqueous buffer to 75% in the presence of lipid vesicles, but remained constant in solutions of β-octyl glucoside. Differential scanning calorimetry (DSC) measured the thermodynamic properties of the unfolding process and was our reference method. The increased heat capacity of the unfolded protein made an important contribution to the total enthalpy of unfolding. The structural properties of Apo A-1 were studied with circular dichroism (CD) spectroscopy. The CD-recorded unfolding transitions were broader than the corresponding DSC transitions and were shifted toward higher temperatures. DSC and CD data were analyzed with the two-state model and the Zimm−Bragg theory. The two-state model assumes just two species in solution, native (N) and unfolded (U) Apo A-1. However, Apo A-1 unfolding is a highly cooperative event with helical amino acid residues unfolding and refolding rapidly. For such a sequential process, the Zimm−Bragg theory provides an alternative and physically more realistic model. The Zimm−Bragg theory allowed perfect simulations of the DSC and CD experiments. In contrast, incorrect thermodynamic results were obtained with the two-state model. The Zimm−Bragg theory also provided a physically well-defined analysis of the cooperativity of the folding ⇄ unfolding equilibrium. The cooperative unfolding of Apo A-1 increased upon addition of lipids and decreased in detergent solution.

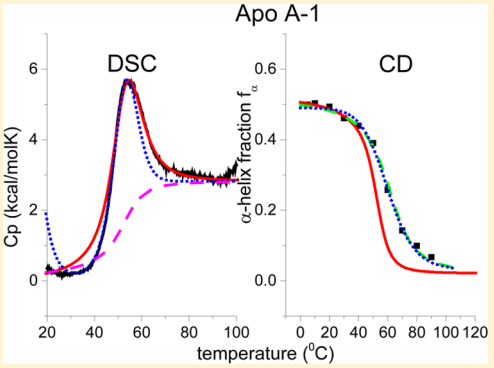

Temperature-induced unfolding of proteins gives insight into the stability of proteins and their structural and functional properties. In view of the increasing potential of proteins in medical applications, quantitative methods to assess their stability in high concentration solutions are of particular interest.

Optical techniques are commonly used to investigate protein folding ⇄ unfolding transitions. Circular dichroism (CD) spectroscopy is particularly important and can be used to measure changes in the overall secondary structure as a function of temperature or solvent conditions. The thermodynamic aspects of protein unfolding are accessible with differential scanning calorimetry (DSC). Protein unfolding entails a disruption of various noncovalent interactions such as hydrogen bonds, salt bridges, or van der Waals interactions and leads to binding of additional water. These changes are reflected in a temperature-dependent increase of the molar heat capacity $C_p(T)$. The heat capacity vs temperature curve provides a quantitative measure of the progress of the unfolding reaction. The total unfolding enthalpy can be derived from the area under the curve.

Protein unfolding is generally assumed to follow a two-state equilibrium between a native (N) and an unfolded (U) conformational state.[1] If the unfolding curve cannot be described by a single transition, a superposition of several two-state curves is applied ("non two-state model"[2]). The advantage of the two-state N ⇄ U model is its mathematical simplicity and its ease of application. On the other hand, it ignores and may even contradict the molecular mechanism of unfolding. Considering the α-helical domains of a protein, the unfolding process is a zipper-like opening of hydrogen bonds. Realistic models describing such sequential effects are provided by the Zimm−Bragg theory[3−5] and the Lifson−Roig theory[6] which have been applied to synthetic polypeptides,[4,7−11] but have found only little attention in the area of protein unfolding. Recent advances in helix−coil theory are described in a comprehensive review.[12] A theory for protein folding cooperativity of helix bundles has also been published.[13]

In the present study we compare differential scanning calorimetry and circular dichroism spectroscopy in deriving the thermodynamic parameters of the folding ⇄ unfolding equilibrium of human Apo A-1. Apo A-1 is well suited for such studies as it is a water-soluble, amphipathic protein with a high α-helix content of about 50% at room temperature.[14,15] Full-length Apo A-1 has eluded crystallization so far, but a 2.2-Å crystal structure of a truncated Δ(185−243)Apo A-1 has recently been published.[16] It shows that Δ(185−243)Apo A-1

Received: March 5, 2015
Revised: April 23, 2015
Published: April 24, 2015

DOI: 10.1021/acs.biochem.5b00238
Biochemistry 2015, 54, 3063−3075

forms a half-circle dimer. The backbone of the dimer consists of two elongated antiparallel helices (~80% helix content). The N-terminal domain of each molecule forms a four-helix bundle with the helical C-terminal region of the symmetry-related partner.[16]

The folding ⇄ unfolding transition of full-length Apo A-1 has its midpoint between 50 and 60 °C and is readily measured with both CD spectroscopy and DSC. Five helical domains are located in the N-terminal two-thirds of Apo A-1[17] and about 115 ± 10 amino acid residues participate in the unfolding reaction. Amide backbone hydrogen/deuterium exchange (HDX) experiments provide convincing evidence that the individual helices in Apo A-1 exist transiently, opening and closing within seconds or less.[15,17] Apo A-1 also undergoes reversible association with maximum oligomer formation at 22 °C and almost complete dissociation at 45 °C.[18−25] The association−dissociation equilibrium does not interfere with the thermodynamics of protein unfolding.[23]

We used highly purified recombinant human Apo A-1 with an N-terminal gly-gly extension. Apo A-1 was measured at concentrations of 10−160 μM in aqueous buffer, in solutions of the nonionic detergent β-octyl glucoside, and in the presence of small unilamellar phospholipids vesicles (SUVs). Unfolding transitions were recorded with DSC and CD spectroscopy, and the folding ⇄ unfolding equilibrium was analyzed with the Zimm−Bragg theory and the two-state model. The thermal unfolding of Apo A-1 has been described almost exclusively with the two-state model by others[26−30] and only recently with the Zimm−Bragg theory by us.[23]

MATERIALS AND METHODS

Apolipoprotein A-1 (Apo A-1). Recombinant preparation and purification of Apo A-1 have been described before.[23] Stock solutions (10.5 mg/mL in PBS buffer) were dialyzed against 150 mM NaCl, 10 mL sodium phosphate, pH 7.4 (PBS buffer) or 100 mM NaF, pH adjusted to pH 7.2 with 20% HCl (NaF buffer), and diluted to the appropriate concentration.

The sequence of purified recombinant human Apo A-1 (termed "Apo A-1" in the following) differed from the human wild-type sequence by two additional N-terminal glycine residues. Electrospray mass spectrometry revealed a molecular mass of 28192.3 Da (the theoretical value for human Apo A-1 with two Gly residues is 28192.7 Da).The protein concentration was determined by measuring the optical density at 280 nm using an extinction coefficient of ε = 32 422 M^{-1} cm^{-1}. About 50 CD experiments and an equal number of DSC experiments, not counting the various controls, were made with the same batch of highly purified Apo A-1.

In our hands the "aggregation propensity" of purified recombinant ApoA1 was very low. Our purification protocol involves steps where the protein is denatured with 6 M guanidine HCl. Removal of the denaturant in a subsequent renaturation step was never a problem. We did not lose significant amounts of ApoA1 due to aggregation. This also reflects high stability of the correctly folded molecular structure of ApoA1.

Contradictory reports from the literature may be explained by endotoxins that might have contaminated those specific ApoA1 preparations. Bacterial endotoxins bind very strongly to ApoA1 and by that its physicochemical properties get changed. The quantitative removal of endotoxins from ApoA1, which we achieved with our purification protocol, is by far not trivial.

Preparation of Lipid Vesicles. POPC was dried from a stock solution in chloroform by a gentle stream of nitrogen followed by a high vacuum overnight. The dried POPC was weighed, and a defined volume of POPG stock solution in chloroform was added to yield a POPC/POPG molar ratio of 3:1. After mixing, the solvent was removed under a gentle stream of nitrogen, and the thin lipid film was exposed to high vacuum overnight and weighed again. The lipids were suspended in PBS buffer with vortex mixing, leading to multilamellar vesicles (MLVs) with a final lipid concentration of 10−20 mM. Small unilamellar vesicles (SUVs) for DSC and CD measurements were prepared by sonication of the lipid suspension using a titanium tip ultrasonicator (Branson Sonifier, Danbury, CT) for 20 min until an almost clear solution was obtained. The solution was cleared by centrifugation for 2 min in an Eppendorf 5415C benchtop centrifuge (Vaudaux-Eppendorf AG, Schoenenbuch, Switzerland).

Differential Scanning Calorimetry (DSC). Starting at 10 or 25 °C, the thermal unfolding of lipid-free and lipid-bound Apo A-1 was measured by increasing the temperature to 90 or 110 °C. DSC experiments were performed with a VP-DSC instrument (Microcal, Northampton, MA). Protein solutions were degassed, and the reference cell was filled with buffer. The heating rate was 1 °C/min. The cell volume was 0.5194 mL. The evaluation of the DSC curves will be described in more detail below. The folding ⇄ unfolding transitions were completely reversible for solutions not heated higher than 90 °C.

Circular Dichroism (CD). CD measurements of Apo A-1 in the absence or presence of POPC:POPG (75:25) small unilamellar vesicels (SUV) were done with a Chirascan CD spectrometer (Applied Photophysics Ltd., Leatherhead, U.K.). Apo A-1 was dissolved at about 10 μM or 100 μM in either NaF or PBS buffer. CD spectra were measured in a quartz cuvette of 1 mm (10 μM Apo A-1) or 0.1 mm (100 μM Apo A-1) path length. The temperature was measured with an electric sensor placed inside the 1 mm cuvette. After heating to 90 °C, the sample was cooled to 25 or 10 °C and measured again. The unfolding process of lipid-free Apo A-1 was completely reversible as the CD spectrum after heating to 90 °C and returning to the starting temperature was virtually identical to the first spectrum. The measurements in 100 mM NaF provided high-quality circular dichroism spectra down to a wavelength of about 190 nm. Because of absorbance of the PBS buffer at low wavelength, the quantitative analysis of the CD spectra was restricted to a wavelength range of 205−250 nm.

The percentage of peptide secondary structure was estimated from a computer simulation based on the reference spectra obtained by Reed and Reed.[31]

Two-State Model Applied to Apo A-1. According to the two-state model, a protein adopts either the native (N) or the unfolded (U) state. The equilibrium N ⇄ U is described with a single, temperature-dependent equilibrium constant $K_N^U(T)$.

$$K_N^U(T) = \frac{[U]}{[N]} = \frac{1 - \Theta_N}{\Theta_N} \quad (1)$$

[N] and [U] denote the equilibrium concentrations of native and unfolded protein, respectively, and $\Theta_N = [N]/([N] + [U])$ is the fraction of native protein. With this definition, a stable protein is characterized by a small equilibrium constant $K_N^U \ll$

DOI: 10.1021/acs.biochem.5b00238
Biochemistry 2015, 54, 3063−3075

1. The temperature-dependent equilibrium constant $K_N^U(T)$ follows the van't Hoff equation

$$\ln \frac{K_2}{K_1} = -\frac{\Delta H_{NU}^0}{R}\left(\frac{1}{T_2} - \frac{1}{T_1}\right) \quad (2)$$

where K_1 = equilibrium constant at temperature T_1, K_2 = equilibrium constant at temperature T_2, and R = universal gas constant.

A plot of $\ln(K_N^U(T))$ versus the reciprocal absolute temperature, $1/T$, yields a straight-line with slope $(-\Delta H_{NU}^0/R)$, if ΔH_{NU}^0 is independent of temperature. ΔH_{NU}^0 is the enthalpy of the conformational change.

The population of the native N and unfolded U state depends on the free energy difference of the unfolding process, $\Delta G_N^U = G_U - G_N$. The relation between the binding constant, $K_N^U(T)$, and the free energy of the transition, $\Delta G_N^U(T)$, is given by

$$\Delta G_N^U(T) = -RT \ln K_N^U(T) \quad (3)$$

The native state is preferentially populated if $\Delta G_N^U(T)$ is positive $(\Delta G_N^U(T) > 0, K_N^U(T) \ll 1)$

The temperature dependence of the free energy is given by

$$\Delta G_N^U(T) = \Delta H_N^U(T) - T\Delta S_N^U(T) \quad (4)$$

where $\Delta S_N^U(T)$ is the unfolding entropy.

At the midpoint of the transition, characterized by the temperature T_0, the equilibrium constant is $K_N^U(T_0) = 1$, the free energy $\Delta G_N^U(T_0) = 0$, and thus $\Delta H_{NU}^0 = T_0\Delta S_{NU}^0$. The free energy of the unfolding process is then simplified to

$$\Delta G_N^U(T) = H_{NU}^0\left(1 - \frac{T}{T_0}\right) \quad (5)$$

and depends on two parameters only. As T_0 is experimentally well-defined, ΔH_{NU}^0 is the only adjustable parameter in the two-state model. The fraction of native protein is then given by

$$\Theta_N = [1 + K_N^U(T)]^{-1} = [1 + e^{-(G_{NU}(T)/RT)}]^{-1} \quad (6)$$

Eq 6 allows the simulation of the DSC and CD unfolding transitions for the complete experimental temperature range.

Zimm–Bragg Theory Applied to Apo A-1. α-Helix folding is fast and occurs on a sub-millisecond time scale.[32,33] Indeed, HDX experiments indicate that the individual helices in Apo A-1 exist transiently, opening and closing within seconds.[15,17,34] The folding ⇄ unfolding equilibrium of Apo A-1 is thus a higly dynamic process, involving a cooperative zipper-like disruption and formation of helical domains. A quantitative analysis of this process is possible with the Zimm–Bragg theory.[3,4,23,35] The theory includes a nucleation parameter, σ, which is temperature-independent, and a temperature-dependent growth parameter, $s(T)$. The nucleation parameter reflects the difficulty of starting an α-helical segment within a stretch of random coil elements. The smaller the value of σ, the steeper is the cooperative transition. Numerical values are in the range of $10^{-3} \geq \sigma \geq 10^{-7}$. The growth parameter, $s(T)$, is the equilibrium constant for the addition of an α-helical segment to an existing α-helix. It entails the formation of an intramolecular hydrogen bond with enthalpy h ($h \approx -1.1$ kcal/mol in aqueous solution[5,11]). The temperature-dependence of $s(T)$ is then given by

$$s(T) = e^{-h/R\left(\frac{1}{T} - \frac{1}{T_\infty}\right)} \quad (7)$$

For a sufficiently long peptide/protein chain with $N \gg \sigma^{-1/2}$ segments, the characteristic temperature, T_∞, is identical to the midpoint, T_0, of the conformational transition. For peptides with a shorter chain length, $N \leq \sigma^{-1/2}$, the characteristic temperature, T_∞, is larger than T_0.

The fourth parameter entering the Zimm–Bragg theory is the chain length, N, defined by the number of amino acid residues involved in the α-helix-to-random coil transition. Short chains of length $N \leq \sigma^{-1/2}$ will exhibit a much broader transition than long chains with $N \gg \sigma^{-1/2}$. Knowledge of the exact number of amino acid residues is hence essential if N is below the cooperative chain length of $N_{coop} = \sigma^{-1/2}$. For a nucleation parameter $\sigma = 10^{-4}$ this cooperative chain length is $N_{coop} = 100$.

A polypeptide chain of N amino acid residues can adopt a maximum of 2^N conformations as each segment can be either coil (c) or helix (h). A polypeptide chain of length i, ending on c or h, can be extended by a h or c segment at position i +1 leading to the combinations cc, hc, ch, and hh. The conditional probabilities of occurrence are summarized in the matrix[35]

$$M = \begin{pmatrix} 1 & \sigma s \\ 1 & s \end{pmatrix} \quad (8)$$

where $s = s(T)$ is given by eq 7. M is used to calculate the partition function Z

$$Z = (1 \quad 0)\begin{pmatrix} 1 & \sigma s \\ 1 & s \end{pmatrix}^N \begin{pmatrix} 1 \\ 1 \end{pmatrix} \quad (9)$$

from which the helix fraction can be calculated

$$\Theta_{helix}(T) = \frac{s}{N}\frac{d(\ln Z)}{dT}\left(\frac{ds}{dT}\right)^{-1} \quad (10)$$

The recombinant human Apo A-1 used in this study has a chain length of 245 amino acids. Its α-helix content in PBS solution without lipid, measured by CD spectroscopy, varies between $f_\alpha \approx 55 \pm 6\%$ at 10 °C and $f_\alpha \approx 8 \pm 5\%$ at 90 °C. The number of amino acid residues involved in the α-helix-to-random coil transition can thus be calculated as $N = 115 \pm 10$ residues.

The Zimm–Bragg theory[3] and the equivalent Lifson–Roig theory[6] have been extended over the years to include specific protein properties. Recent advances have been reviewed.[12] However, the standard Zimm–Bragg theory provides a good fit of all experimental Apo A-1 data and a more elaborate theoretical approach appears not to be necessary.

The Zimm–Bragg theory is based on peptide units classified by their hydrogen bond formation. The h-parameter is usually specified as the hydrogen bonding energy but could have a different molecular origin. Free energy calculations have concluded that "hydrogen bond formation contributes little to helix stability because the internal hydrogen bonding energy is largely cancelled by the large free energy cost associated with removing polar groups from water".[36] "The major driving force favoring helix formation can be associated with interactions including van der Waals interactions in the close-packed helix conformation and the hydrophobic effect".[36] In the light of these calculations the h-parameter could be considered as an empirical parameter for sequential effects making also less

DOI: 10.1021/acs.biochem.5b00238
Biochemistry 2015, 54, 3063–3075

helical proteins amenable to an analysis with the Zimm−Bragg theory.

RESULTS

Differential Scanning Calorimetry of Lipid-Free Apo A-1. Differential scanning calorimetry measures the change of the heat capacity, $C_{p,NU}(T)$, during the unfolding process. $C_{p,NU}(T)$ includes the conformational change of Apo A-1 and also the increased heat capacity of the unfolded protein, $\Delta C^0_{p,NU} = C^0_{p,U} - C^0_{p,N}$, mainly caused by binding additional water molecules. $\Delta C^0_{p,NU}$ contributes significantly to the unfolding enthalpy of proteins[37,38] but was mostly neglected in the evaluation of Apo A-1 unfolding experiments.

A DSC scan of a 71 μM Apo A-1 solution in NaF buffer is displayed in Figure 1A. The maximum of the heat capacity is found at 53.5 °C. After heating to 90 °C the sample was cooled to 25 °C and measured again. The unfolding process of lipid-free Apo A-1 was completely reversible as three consecutive DSC scans were virtually identical.

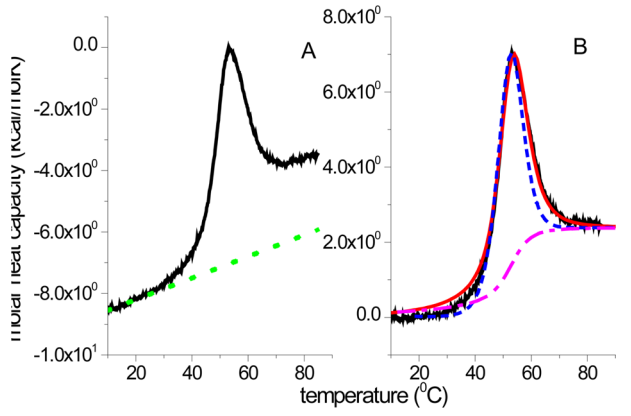

Figure 1. Differential scanning calorimetry (DSC) of 71 μM Apo A-1 in NaF buffer. (A) Black line: DSC scan. Dotted green line: baseline correction. (B) Black line: baseline-corrected DSC scan. Red solid line: best fit with the Zimm−Bragg theory with $\sigma = 9 \times 10^{-5}$, $h = -1100$ cal/mol, $N = 110$, $\Delta C^0_{p,NU} = 2.388$ kcal/mol·K, and $T_\infty = 332.3$ K = 59.15 °C. Dashed blue line: best fit with the two-state model with $\Delta H^0_{NU} = 66.9$ kcal/mol, $T_0 = 324.5$ K = 51.35 °C, and $\Delta C^0_{p,NU} = 2.388$ kcal/mol·K. Dash-dot magenta line: contribution of the heat capacity change $\Delta C^0_{p,NU}$ to the folding ⇄ unfolding transition, calculated with the Zimm−Bragg theory.

The heat capacity difference between the native and the unfolded state is $\Delta C^0_{p,NU} = 2.39$ kcal/mol·K. CD spectra were recorded in parallel and spectral deconvolution showed that 110 amino acid residues were involved in the α-helix-to-random coil transition.

Numerical integration of the experimental $C_{p,NU}(T)$ vs T curve (Figure 1B) from 40 to 70 °C results in a total unfolding enthalpy of $\Delta H^0_{exp} = 123.8$ kcal/mol. This corresponds to an enthalpy change of $h = 1.125$ kcal/mol per amino acid residue. This enthalpy value is characteristic for the opening of an α-helix hydrogen bond in aqueous solution.[7−9,11] The Apo A-1 unfolding enthalpy can thus be assigned almost exclusively to an opening of hydrogen bonds with little contributions from tertiary structure. The averaged results of DSC unfolding experiments of Apo A-1 in aqueous solution, in solutions containing β-octyl glucoside, and bound to lipid bilayers are summarized in Table 1.

Table 1. Thermal Unfolding of Apo A-1 Measured with DSC[a]

	number of experiments	T_0 (°C)	ΔH^0_{exp}, kcal/mol	$\Delta H^0_{calc,ZB}$, kcal/mol	$\Delta H^0_{calc,2\text{-}st}$, kcal/mol	h_{exp}, cal/mol	$\Delta C^0_{p,NU}$, kcal/mol·K	$\Delta H^0_{C_p,ZB}$, kcal/mol	$T_{\infty,ZB}$, °C	σ_{ZB}
100 m NaF pH 7.2 or PBS buffer pH 7.4	6	52.1 ± 0.6	123.7 ± 10.6	127.4 ± 7.4	112.7 ± 1.8	1076 ± 79	2.52 ± 0.09	51.6 ± 1.9	59.3 ± 0.7	$(9.3 \pm 3.3) \times 10^{-5}$
0.05−5 mM β-octyl glucoside in PBS	5	51 ± 0.3	138.2 ± 6.9	141 ± 6.1	117.3 ± 2.7	1133 ± 58	2.72 ± 0.09	58.4 ± 6.8	56.7 ± 1.3	variable[b]
POPC/POPG 3/1 mol/mol	4	87.2 ± 2.9	139.7 ± 13.9	139.7 ± 6.8	120 ± 2.1	792 ± 77	2.21 ± 0.46	45.1 ± 2.9	94.4 ± 2.2	$(3.8 \pm 1.7) \times 10^{-5}$

[a]Experimental results and parameters of the Zimm−Bragg theory and the two-state model. ZB: Zimm−Bragg parameters. 2-st: two-state model. [b]See Table 3.

DOI: 10.1021/acs.biochem.5b00238
Biochemistry 2015, 54, 3063−3075

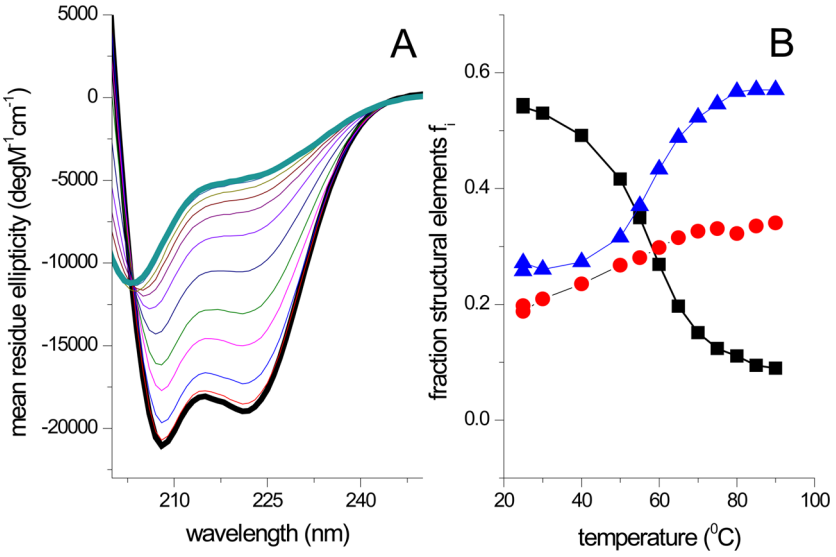

Figure 2. CD spectroscopy of thermal unfolding of 9.7 μM Apo A-1 in NaF buffer. (A) Far-UV CD spectra recorded in 5−10 °C steps from 25 °C (thick black line) to 90 °C (thick blue line). (B) Deconvolution of the CD spectra of panel A in terms of three structural elements: (■) α-helix, (red solid circle) β-sheet + β-turn, and (blue solid triangle) random coil.

The simulation of the DSC scan with the Zimm−Bragg theory is displayed in Figure 1B (solid red line). An excellent fit of the folding ⇄ unfolding transition is obtained. The calculated unfolding enthalpy $\Delta H^0_{\mathrm{calc,ZB}}$ = 127.7 kcal/mol is in very good agreement with the experimental result. The predicted midpoint of the α-helix-to- random coil transition (Θ_{helix} = 0.5) is at T_0 = 51 °C, that is, 2.5 °C below the maximum of the C_p(T) curve (see also Discussion).

As mentioned above, $\Delta H^0_{\mathrm{exp}}$ includes both the enthalpy of the conformational change, ΔH^0_{NU}, and the enthalpy change $\Delta H^0_{C_p,\mathrm{NU}}$ caused by the heat capacity increase, $\Delta C^0_{p,\mathrm{NU}}$, of the unfolded protein. An experimental separation of the two enthalpies is not possible but can be deduced with the Zimm−Bragg theory or the two-state model. The dash-dot magenta line in Figure 1B shows the temperature-dependence of the heat capacity $\Delta C_{p,\mathrm{NU}}$ calculated with the Zimm−Bragg theory according to

$$\Delta H^0_{C_p,\mathrm{NU}} = (1 - Q_{\mathrm{N}}(T))\Delta C^0_{p,\mathrm{NU}} \qquad (11)$$

$\Theta_{\mathrm{N}}(T)$, the fraction of native protein, can be calculated with either the two-state model or the Zimm−Bragg theory. The corresponding enthalpy is defined by the area under this curve and amounts to $\Delta H^0_{C_p,\mathrm{ZB}}$ = 49.0 kcal/mol, accounting for ∼40% of the total unfolding enthalpy. $\Delta C^0_{p,\mathrm{NU}}$ leads to an asymmetric unfolding transition in the DSC experiment which explains the temperature difference between the C_p(T) maximum and the midpoint of the α-helix-to-random coil transition.

The best fit of the DSC transition curve calculated with the two-state model is also included in Figure 1B (dashed blue line). The conformational enthalpy ("van't Hoff enthalpy"), ΔH^0_{NU}, is the primary input parameter and was found to be ΔH^0_{NU} = 66.9 kcal/mol, in excellent agreement with literature data.[26,27] ΔH^0_{NU} was used to calculate the contribution of the heat capacity term $\Delta C^0_{p,\mathrm{NU}}$ resulting in $\Delta H^0_{C_p,\text{2-state}}$ = 38.5 kcal/mol. The total enthalpy was therefore $\Delta H^0_{\mathrm{calc,2\text{-}state}}$ = 105.4 kcal/mol, which is ∼20% smaller than the experimental value. Visual comparison of the two-state best fit with the experimental data reveals that the high-temperature end of the folding ⇄ unfolding transition of Apo A-1 is not well described by the two-state model.

Thermal Unfolding of Lipid-Free Apo A-1 Measured with CD Spectroscopy. CD spectra of Apo A-1 (9.7 μM) in NaF buffer recorded as a function of temperature are shown in Figure 2A. Thick lines indicate spectra with the highest (25 °C, black) and the lowest (90 °C, blue) α-helix content. The analysis of the CD spectra in terms of secondary structures is shown in Figure 2B. The α-helix fraction decreases from f_α = 54% at 25 °C to 9% at 90 °C. The recombinant glygly-Apo A-1 has a chain length of 245 amino acids and the loss of helical amino acid residues is thus ΔN = 0.45 × 245 = 110 residues. The midpoint of the folding ⇄ unfolding transition was at T_0 = 55.7 °C, that is, 4.7 °C higher than that obtained from the DSC unfolding transition. The random coil structure increases from f_{rc} = 26% to 57% and the β-structure (β-sheet + β-turn) from f_β = 20% to 34%. As a consequence of the β-structure increase, the isodichroic point seen in Figure 2A is not exact as can be verified by a high resolution presentation of the region around 203 nm (not shown). The existence of β-structures in Apo A-1 has mostly been ignored in previous investigations. However, EPR experiments have led to the conclusion that about 11% of Apo A-1 is organized in β-strands.[39,40]

The folding ⇄ unfolding equilibrium as reflected in the α-helix fraction f_α (Figure 2B) was analyzed with the Zimm−Bragg theory (Figure 3, solid red line). An excellent fit of the CD transition curve was obtained; however, the cooperativity parameter $\sigma = 1 \times 10^{-3}$ was by a factor of 10 larger (lower cooperativity) than that of the DSC unfolding transition.

Next, eq 6 was used to fit the CD transition curve with the two-state model (dashed blue line in Figure 3) also yielding a good fit with T_0 = 55.7 °C (identical with the result of the Zimm−Bragg theory) but a van't Hoff enthalpy of $\Delta H^0_{\mathrm{NU,CD}}$ = 29.6 kcal/mol,

The latter value is in agreement with earlier findings[28,41−43] but is much smaller than $\Delta H^0_{\mathrm{NU,DSC}}$ = 66.9 kcal/mol, deduced with the same two-state model from the DSC data, and obviously far different from the true heat of unfolding. Both the Zimm−Bragg theory and the two-state model therefore indicate significant differences between the calorimetric and spectro-

DOI: 10.1021/acs.biochem.5b00238
Biochemistry 2015, 54, 3063−3075

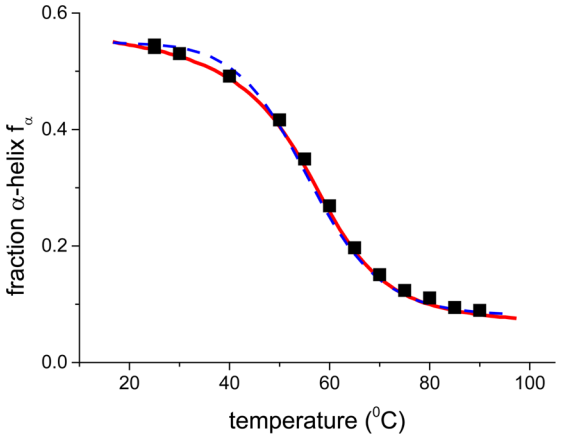

Figure 3. Analysis of the unfolding transition of Figure 2B with the Zimm–Bragg theory and the two-state model. (■) α-helix fraction, experimental results (same as in Figure 2B) . Red solid line: α-helix content calculated with the Zimm–Bragg theory. $\sigma = 1 \times 10^{-3}$, $h = -1100$ cal/mol, characteristic temperature $T_\infty = 333.5$ K, number of amino acid residues participating in the α-helix-to-random coil transition $N = 110$. Dashed blue line: α-helix fraction calculated with the two-state model. Unfolding enthalpy $\Delta H^0_{NU} = 29.6$ kcal/mol. The midpoint temperature of the transition is $T_0 = 55.7$ °C ($f_\alpha = 0.325$).

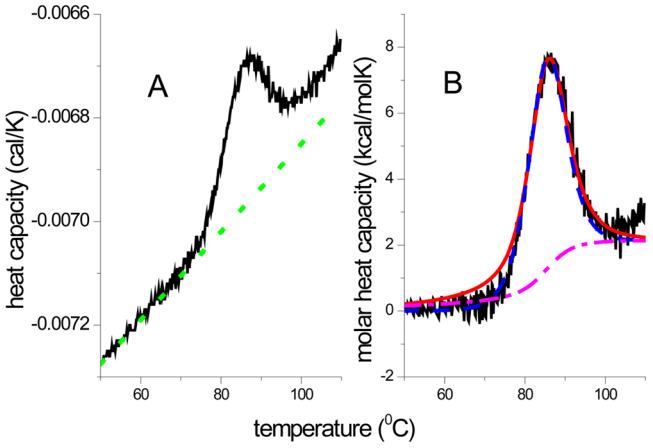

Figure 4. DSC of lipid-bound Apo A-1. 71 μM Apo A-1 solution in 40 mM phospholipid vesicles (POPC/POPG, 3:1 mol: mol) SUVs. (A) Black line (–): DSC scan. Dotted green line: baseline correction. (B) Black line (–): DSC scan. Red solid line: Zimm–Bragg model with $\sigma = 2 \times 10^{-5}$, $h = -800$ cal/mol, $N = 175$, and $\Delta C^0_{p,NU} = 2.15$ kcal/mol·K, and $T_\infty = 366$ K = 92.85 °C. The midpoint of the α-helix-to-random coil transition is at $T_0 = 84.6$ °C. Dashed blue line: two-state model with $\Delta H^0_{NU} = 80.0$ kcal/mol, $T_0 = 357.6$ K = 84.6 °C, and $\Delta C^0_{p,NU} = 2.15$ kcal/mol·K. Dash-dot magenta line: contribution of the heat capacity $\Delta C^0_{p,NU}$ to the unfolding enthalpy.

scopic measurements of the folding ⇄ unfolding equilibrium of Apo A-1.

The evaluation of the CD spectra and the parameters of the Zimm–Bragg theory and two-state model are summarized in Table 2.

Differential Scanning Calorimetry of Apo A-1 Bound to Lipid Vesicles. Apo A-1 (71 μM) was incubated with 40 mM phospholipid vesicles (POPC/POPG, 3:1 mol/mol) in PBS buffer (lipid-to-protein molar ratio ≈ 570). The DSC scan is shown in Figure 4A before and in Figure 4B after baseline correction. The molar heat capacity of Apo A-1 increased upon unfolding by $\Delta C^0_{p,NU} = 2.15$ kcal/mol·K, which is similar to the result observed for lipid-free Apo A-1.

The midpoint of the unfolding transition was found at 84.7 °C, that is, 33 °C higher than the midpoint of lipid-free Apo A-1 unfolding. CD spectroscopy showed that about 175 amino acids residues participated in the folding ⇄ unfolding transition. Unexpectedly, the heat of unfolding $\Delta H^0_{exp} = 124.9$ kcal/mol was almost identical to that observed for lipid-free Apo A-1. Referred to 175 amino acid residues the hydrogen bond enthalpy was reduced to $h = -0.714$ kcal/mol. This appears to be a consequence of the more hydrophobic environment of Apo A-1 in the lipid membrane. A value of $h = -0.7$ kcal/mol was reported for α-helix formation in trifluoroethanol (TFE)–water mixtures.[44] Similarly, α-helix formation of the antibacterial peptide magainin at the membrane surface was characterized by $h = -0.7$ kcal/mol per residue.[45]

The simulation of the DSC transition curve with the Zimm–Bragg theory (red line in Figure 4B) results in an excellent fit of the folding ⇄ unfolding transition. The calculated heat of unfolding for the temperature interval defined above is $\Delta H^0_{calc,ZB} = 130.6$ kcal/mol, in good agreement with the experimental result.

The dashed magenta line in Figure 4B represents the contribution of the heat capacity term $\Delta C^0_{p,NU}$ to the total unfolding enthalpy, yielding $\Delta H^0_{C_p,ZB} = 45.8$ kcal/mol.

The DSC unfolding transition was simulated equally well with the two-state model. The conformational enthalpy was $\Delta H^0_{NU,2\text{-state}} = 80.0$ kcal/mol, and the contribution of the $\Delta C^0_{p,NU}$ term was $\Delta H^0_{C_p,2\text{-state}} = 41.1$ kcal/mol. The resulting total unfolding enthalpy was therefore $\Delta H^0_{calc,2\text{-state}} = 121.1$ kcal/mol.

The DSC scans of lipid-bound Apo A-1 were only partially reversible probably because the solution was heated to the higher temperature of 110 °C. The second DSC scan of the same Apo A-1-lipid sample showed a downward shift of the transition maximum to $T_0 = 79$ °C, a 10% increase in the transition enthalpy, and a 30% increase in the molar heat

Table 2. Thermal Unfolding of Apo A-1 Measured with CD Spectroscopy[a]

	# of exp	$T_{\Theta=0.5}$, °C	Θ_{max}	Θ_{min}	ΔN_{helix}	$T_{\infty,ZB}$, °C	σ_{ZB}	h_{ZB}, cal/mol	$\Delta H^0_{NU,2\text{-st}}$, kcal/mol
PBS buffer, 100 mM NaF	6	56.4 ± 1.1	0.55 ± 0.06	0.08 ± 0.05	115 ± 3	60.6 ± 1.4	$(9.3 \pm 3.1) \times 10^{-4}$	−1100	28.4 ± 1.9
0.05–10 mM β-octyl glucoside[b]	14	58.3 ± 2.4	0.51 ± 0.05	0.04 ± 0.02	116 ± 10	63.5 ± 2.9	$(7.8 \pm 2.4) \times 10^{-4}$[b]	variable[b]	25.6 ± 2.7[b]
POPC/POPG 3/1	2	88.6 ± 2.2	0.72 ± 0.04	0.03 ± 0.02	170 ± 5	88.5 ± 0.5	$(7.5 \pm 2.5) \times 10^{-4}$	−800	19.1
POPC	1	78	0.8	0.02	191	79	8×10^{-4}	−800	23.9

[a]Experimental results and simulation parameters of the Zimm–Bragg theory and the two-state model.. ZB: Zimm Bragg parameter. 2-st: two-state model. [b]See Table 3.

DOI: 10.1021/acs.biochem.5b00238
Biochemistry 2015, 54, 3063–3075

capacity of the unfolded protein. The third scan was similar to the second.

CD Spectroscopy of Apo A-1 Bound to Lipid Vesicles. Temperature-dependent CD spectra of lipid-bound Apo A-1 are shown in Figure 5A. The α-helix content at room

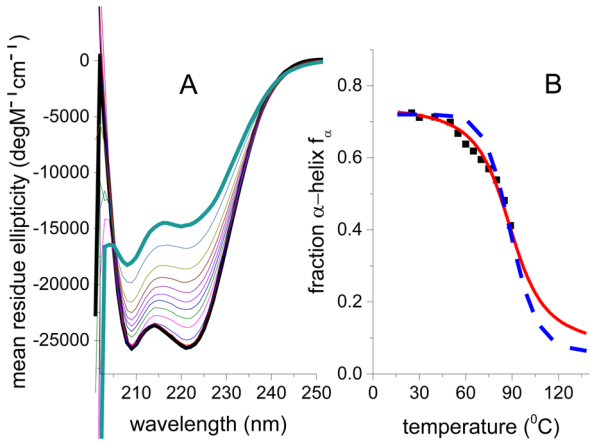

Figure 5. CD spectroscopy of thermal unfolding of Apo A-1 (10 μM) in NaF buffer bound to phospholipid vesicles (6 mM). POPC/POPG, 3:1 mol:mol. (A) Far-UV CD spectra recorded in 5−10 °C steps between 25 °C (black line) and 89 °C (blue line). Below 203 nm the CD spectra become distorted due to light scattering by lipid vesicles. (B) (■) α-Helix fraction derived by deconvolution of CD spectra. Solid red line: Zimm−Bragg theory with $\sigma = 1.0 \times 10^{-3}$, $h = -800$ cal/mol, $N = 175$ and $T_\infty = 362.15$ K = 89 °C. The predicted midpoint of the transition is also at $T_0 = 89$ °C. The dashed blue line is the prediction of the two-state model calculated with $\Delta H^0_{NU} = 29.6$ kcal/mol and $T_0 = 89$ °C.

temperature increases from 53% for lipid-free to 72% for lipid-bound Apo A-1, in agreement with earlier reports.[14] Upon heating the α-helix content decreases from 72% at 25 °C to 36% at 89 °C, which is about the midpoint of the DSC transition (Figure 5B). Higher temperatures were not accessible due to technical limitations of the CD instrument. The fraction of β-sheet structure remained almost constant at $f_\beta \approx 20\%$ throughout the complete temperature range.

The Zimm−Bragg analysis of the CD recorded folding ⇄ unfolding transition of lipid-bound Apo A-1 is shown in Figure 5B (red line; $h = 800$ cal/mol). The α-helix fraction of the denatured Apo A-1 is assumed to be identical to that of lipid-free denatured Apo A-1. The nucleation parameter $\sigma = 1 \times 10^{-3}$ is identical to that of lipid-free Apo A-1 CD transition curve but is 50 times larger than $\sigma = 2 \times 10^{-5}$ as deduced from the DSC transition.

The blue line in Figure 5B represents the best fit obtained with the two-state model. The van't Hoff enthalpy $\Delta H^0_{NU,2\text{-st}} = 29.6$ kcal/mol is identical to that used for CD analysis of lipid-free Apo A-1 but very different from the calorimetric result obtained for lipid-bound Apo A-1.

As already noted for lipid-free Apo A-1, calorimetry and CD spectroscopy of lipid- bound Apo A-1 lead to significantly different results. The folding ⇄ unfolding transition of lipid-bound Apo A-1 is clearly broader and less cooperative in CD spectroscopy than in DSC.

Thermal Unfolding of Apo A-1 Dissolved in β-Octyl Glucoside. Nonionic detergents are suggested to act as membrane-mimicking solvents. We therefore investigated the question of how the addition of β-octyl glucoside could influence the thermodynamic properties of Apo A-1. The protein was dissolved in PBS buffer containing β-octyl glucoside at concentrations of 0 mM $\leq c_{\beta-OG} \leq$ 37 mM. The critical micellar concentration (CMC) of β-octyl glucoside has a minimum of 20.6 mM at 40 °C.[46]

Figure 6A shows the temperature-dependence of the α-helix fraction, f_α, of Apo A-1 for four different concentrations of β-

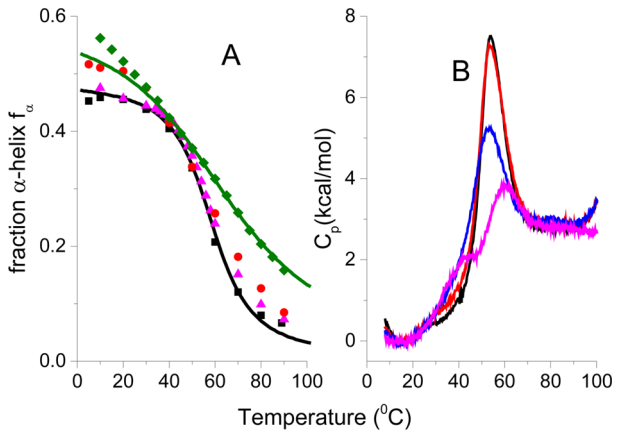

Figure 6. Apo A-1 (100 μM) in PBS buffer containing β-octyl glucoside. (A) CD spectroscopy. α-Helix fraction obtained by deconvolution of CD spectra. (■) 0 mM; (pink solid triangle) 10 mM; (red solid circle) 20 mM; (green solid diamond) 37 mM β-octyl glucoside. Solid lines: predictions of the Zimm−Bragg theory. Black line: 0 mM β-octyl glucoside, $h = -1100$ cal/mol, $N = 120$, $\sigma = 1.0 \times 10^{-3}$, $T_\infty = 335$ K = 61.8 °C. Olive line: 37 mM β-octyl glucoside, $h = -950$ cal/mol, $N = 140$, $\sigma = 1.0 \times 10^{-2}$, $T_\infty = 339$ K = 65.8 °C. (B) Molar heat capacity measured by DSC. Black line: 0 mM; orange line: 1 mM; blue line: 5 mM; magenta line: 10 mM β-octyl glucoside.

octyl glucoside. The CD spectra reveal a pronounced broadening of the transition curves with increasing concentration of β-octyl glucoside. The α-helix content at 10 °C is constant at $f_\alpha = 0.52 \pm 0.05$ for $c_{\beta\text{-OG}} \leq 20$ mM and increases to $f_\alpha = 0.56$ above the CMC. At 90 °C the α-helix content is $f_\alpha = 0.07 \pm 0.03$ for $c_{\beta\text{-OG}} \leq 20$ mM and $f_\alpha = 0.15$ for $c_{\beta\text{-OG}} = 37$ mM. The average number of protein amino acid residues involved in the α-helix-to-random transition is N = 116 ± 10. The midpoint of the CD transition is 58 °C for $c_{\beta\text{-OG}} \leq 10$ mM and shifts to 64 °C for $c_{\beta\text{-OG}} = 37$ mM.

The solid lines in Figure 6A are the predictions of the Zimm−Bragg theory for 0 mM and 37 mM β-octyl glucoside. The nucleation parameter increases by about 1 order of magnitude from $\sigma = 1.0 \times 10^{-3}$ at 0 mM to 1.0×10^{-2} at 37 mM β-octyl glucoside indicating a considerable reduction in cooperativity.

After measurement at 90 °C, the protein solutions were cooled down in 10 °C steps. The CD spectra at same temperatures of the heating and cooling process were found to be identical. On the basis of the CD spectra, the temperature-induced folding ⇄ unfolding transition in β-octyl glucoside appears to be completely reversible.

DSC measurements were performed under conditions identical to those of the CD experiments regarding Apo A-1 concentration and buffer conditions. DSC is more sensitive to a change in detergent concentration than CD spectroscopy (Figure 6B). At $c_{\beta\text{-OG}} = 1$ mM, the DSC curve is almost identical to that of Apo A-1 in detergent-free buffer. At $c_{\beta\text{-OG}} =$ 5 mM the transition becomes broader, and the height of the

DOI: 10.1021/acs.biochem.5b00238
Biochemistry 2015, 54, 3063−3075

$C_{p,NU}(T)$ maximum is reduced. Apo A-1 unfolding in 10 mM β-octyl glucoside even shows two transitions. At 20 mM and 37 mM β-octyl glucoside the DSC curves no longer display a maximum. Instead, the molar heat capacity increases quite dramatically (data not shown). The enthalpy change is now dominated by the dissociation of β-octyl glucoside micelles.[47] Up to 10 mM β-octyl glucoside and 90 °C, the DSC scans were found to be completely reversible.

The DSC unfolding of Apo A-1 in 10 mM β-octyl glucoside is unique as it displays two separate unfolding transitions. The low-temperature transition has its maximum at 41 °C, the main transition at 60.5 °C. Figure 7 shows simulations of the two

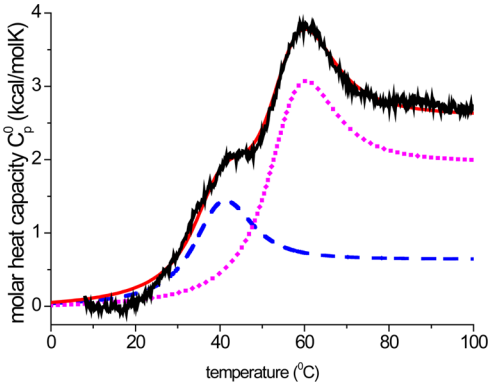

Figure 7. Differential scanning calorimetry of Apo A-1 (100 μM) in PBS buffer with 10 mM β-octyl glucoside. The baseline-corrected heat capacity curve shows two maxima, the first at 41 °C, the second at 60.5 °C. The experimental result (black line) can be simulated by the superposition of two separate transitions calculated with the Zimm–Bragg theory (h = −0.95 kcal/mol, $\sigma = 3.2 \times 10^{-4}$, N = 120). The solid red line is the superposition of the pretransition (dashed blue line) and main transition (dotted magenta line).

folding ⇄ unfolding equilibria with the Zimm–Bragg theory. The unfolding entails an increase in the molar heat capacity, which in the first step is $\Delta C^0_{p,NU}$ = 0.63 kcal/mol·K and in the second $\Delta C_{p,NU}$ = 1.96 kcal/mol·K. The total molar heat capacity change is thus $\Delta C^0_{p,NU}$ = 2.59 kcal/mol·K.

The integration of the experimental unfolding curve from 20 to 80 °C yields a total unfolding enthalpy of ΔH^0_{exp} = 133.2 kcal/mol, which can be divided into $\Delta H^0_{calc,ZB}$ = 47.1 kcal/mol for the pretransition and $\Delta H^0_{calc,ZB}$ = 87.6 kcal/mol for the main transition. The pretransition accounts for ∼35% of the total enthalpy, the main transition for ∼65%. Related to N = 116 ± 10 amino acid residues involved in the α-helix-to-random coil transition 30–40 hydrogen bonds are broken in the pretransition and 80–90 bonds in the main transition.

The DSC and CD measurements with β-octyl glucoside are summarized in numerical form in Table 3.

DISCUSSION

The 2.2-Å crystal structure of truncated Δ(185–243)Apo A-1 shows a dimer of two elongated antiparallel helices with a helix content of about 80%.[16] The helix content of full-length Apo A-1 in solution is 50% and increases to about 80% upon lipid binding. The high helix content of Apo A-1 in solution as well as in the crystal structure of truncated Δ(185–243)Apo A-1 strongly suggests that the thermal unfolding of Apo A-1 should be described by the helix-random coil theory.

The present literature on protein unfolding is dominated by the two-state model. However, as suggested by Doig:[12] "Peptides that form helices in solution do not show a simple two-state equilibrium between a fully folded and fully unfolded structure. Instead they form a complex mixture of all helix, all coil or, most frequently, central helices with frayed coil ends. In order to interpret experiments on helical peptides and make theoretical predictions on helices, it is therefore essential to use a helix–coil theory that considers every possible location of the helix within a sequence."[12] and "The simplest way to analyse the helix–coil equilibrium, still occasionally observed, is the two-state model, in which the equilibrium is assumed to be between 100% helix conformation and 100% coil. This is incorrect and its use gives serious errors. This is because helical peptides are generally most often found in partly helical conformations, often with a central helix and frayed disordered ends, rather than in the fully folded or fully unfolded states."[12] The specific question of the cooperativity of helix-bundles has been addressed by Ghosh and Dill and was analyzed with a cooperative model quite different from the two-state model.[13]

The focus of the present study is thermal unfolding of human Apo A-1 at 50 to 60 °C in aqueous solution and at 85–90 °C in a lipid environment. Our DSC and CD experiments address three different topics: (i) applicability and quality of results of the Zimm–Bragg theory and two-state model when analyzing same DSC and CD transition curves; (ii) thermodynamic insights provided by differential scanning calorimetry of lipid-free Apo A-1; (iii) folding ⇄ unfolding thermodynamics of Apo A-1 in the presence of lipids and nonionic detergents.

Comparison of Methods and Models. The specific differences between DSC and CD spectroscopy are best illustrated with an experimental example (Figure 8). Apo A-1 samples of the same composition were measured with DSC and CD spectroscopy in PBS buffer containing 5 mM β-octyl glucoside. The calorimetric results are reproduced in Figure 8A, and the spectroscopic data are in Figure 8B.

The calorimetric unfolding transition (Figure 8A; black line) has its maximum at 54.5 °C and an unfolding enthalpy of ΔH^0_{exp} = 131.5 kcal/mol. The Zimm–Bragg theory provides an excellent fit of the unfolding transition (Figure 8A, solid red line) with $\Delta H^0_{calc,ZB}$ = 135.0 kcal/mol. The two-state model predicts a DSC transition of smaller width (dotted blue line), a conformational (van't Hoff) enthalpy ΔH^0_{NU} = 52.5 kcal/mol, and a total enthalpy $\Delta H^0_{calc,2\text{-state}}$ = 117.6 kcal/mol, when the change in heat capacity $\Delta C^0_{p,NU}$ = 2.82 kcal/mol·K is included. The predicted enthalpy $\Delta H^0_{calc,2\text{-state}}$ is about 10% smaller than the experimental result. In fact, as a general conclusion it follows from our DSC studies that the two-state model predicts unfolding enthalpies that are 10–20% smaller than the experimental values (see Table 1) and that the conformational enthalpy accounts for only 50–60% of the total enthalpy.

It should also be noted that the $C_p(T)$ maximum (at 54.5 °C in Figure 8A) is not identical with the midpoint (Θ_N = 0.5) of the folding ⇄ unfolding equilibrium (predicted at 50.7 °C by both Zimm–Bragg theory and two-state model). This is a consequence of the $\Delta C^0_{p,NU}$ term which generates an asymmetric conformational transition.

Figure 8B shows the α-helix fraction (filled black squares) of the same protein solution measured with CD spectroscopy. The α-helix content decreased from 52% at 10 °C to about 2% at 90 °C and N = 123 amino acid residues were calculated to participate in the unfolding transition. The midpoint of the experimental transition curve is now at T_0 = 59.9 °C, shifted by 5.5 °C compared to the C_p maximum of the DSC transition.

DOI: 10.1021/acs.biochem.5b00238
Biochemistry 2015, 54, 3063–3075

Table 3. Unfolding of Apo A-1 in β-Octyl Glucoside

Differential Scanning Calorimetry												
c_{pep}, μM	c_{OG}, mM	Lsm	$T_{\Theta=0.5}$	ΔH^0_{exp}, kcal/mol	$\Delta H^0_{calc,ZB}$, kcal/mol	$\Delta H^0_{calc,2\text{-}st}$, kcal/mol	ΔC_p, kcal/mol·K	$\Delta H^0_{C_p,ZB}$, kcal/mol	$T_{\infty,ZB}$, °C	σ_{ZB}	h_{ZB}, cal/mol	N_{ZB}
103	10[a]	PBS, main transition	55	133.5	85.5	nd	1.959	51.7	61.0	3.0×10^{-4}	−950	120
		pretransition	37.5		46.4	nd	0.633	26.2	43.3	3.0×10^{-4}	−950	120
100	10[a]	PBS, main transition	53.6	132.0	77.9	nd	1.959	44.8	59.9	3.0×10^{-4}	−950	120
		pretransition	35.6		52.3	nd	0.633	25	41.2	3.0×10^{-4}	−950	120
100	5	PBS	50.9	131.5	135.0	117.6	2.818	71.5	55.9	3.0×10^{-4}	−1069	123
100	1	PBS	50.9	138.9	142	114.7	2.699	55.4	56.0	2.1×10^{-4}	−1068	130
96	0.2	PBS	50.6	151.2	152.5	120.4	2.842	58.6	55.2	3.4×10^{-4}	−1163	130
100.4	0.1	PBS	51.4	135.5	136.1	115.3	2.627	53.2	57.9	1.4×10^{-4}	−1148	118
101	0.05	PBS	51.4	134.0	136.3	115.3	2.627	53.4	58.7	1.3×10^{-4}	−1218	110

Circular Dichroism Spectroscopy									
c_{pep}, μM	c_{OG}, mM	Lsm	$T_{(\Theta=0.5)}$, °C	Θ_{max}	Θ_{min}	$T_{\infty,ZB}$, °C	σ_{ZB}	h_{ZB}, cal/mol	ΔN_{exp}	$\Delta H_{NU,2\text{-}state}$, kcal/mol
10.3	37	100 mM NaF	55.9	0.63	0.05	59.05	1.0×10^{-2}	−950	142	10.75
10.9	37	H_2O	59.1	0.62	0.07	62.85	7.0×10^{-3}	−950	135	10.75
99	20	PBS	58.1	0.56	0.01	61.85	3.0×10^{-3}	−950	135	19.1
9.7	19	H_2O	60.8	0.54	0.02	64.85	3.0×10^{-3}	−950	127	14.31
103	10	PBS	60.1	0.5	0.02	64.85	1.2×10^{-3}	−950	118	22.69
100	10	PBS	59.6	0.5	0.01	65.35	1.2×10^{-3}	−950	120	23.9
100	10	PBS	59.4	0.5	0.04	65.85	6.0×10^{-4}	−950	113	23.9
104	10	PBS	54	0.55	0.03	58.85	6.0×10^{-4}	−950	127	26.3
10.4	9.5	H_2O	61.4	0.53	0.07	67.35	7.0×10^{-4}	−950	113	22.7
9.7	7.5	H_2O	61.3	0.51	0.05	67.85	4.0×10^{-4}	−950	113	28.66
100	5	PBS	59.9	0.52	0.02	64.35	8.0×10^{-4}	−1100	123	31.05
10.4	1	H_2O	60.3	0.41	0.02	66.35	6.0×10^{-4}	−1100	96	28.66
100	1	PBS	57.9	0.6	0.06	61.85	7.0×10^{-4}	−1100	132	26.27
11	0.2	PBS	56.7	0.48	0.05	61.9	9.0×10^{-4}	−1100	105	26.3
96	0.2	PBS	57.9	0.59	0.06	61.9	8.0×10^{-4}	−1100	130	23.88
10.5	0.1	PBS	55.8	0.48	0.05	60.9	8.0×10^{-4}	−1100	105	26.27
100.4	0.1	PBS	57.1	0.51	0.03	61.4	1.0×10^{-3}	−1100	118	21.49
11	0.05	PBS	55	0.49	0.05	59.85	9.0×10^{-4}	−1100	108	26.3
			58.3[c]	**0.51**[c]	**0.04**[c]	**63.5**[c]	**7.8×10^{-4}**[c]		**115.7**[c]	**25.6**[c]
			2.35	**0.05**	**0.02**	**2.87**	**2.3×10^{-4}**		**10.36**	**2.7**

[a]Two transitions (see Figure 7). [b]Average 0.05−5 mM β-octylglucoside. [c]Average 0.05−10 mM β-octylglucoside.

Application of the two-state model to the CD data results in an excellent fit (Figure 8B, dotted blue line) with a conformational enthalpy (van't Hoff enthalpy) of $\Delta H^0_{NU,2\text{-state}}$ = 30.05 kcal/mol, close to the enthalpies reported above for CD unfolding transitions without detergent and also found in the literature.[28,41−43] However, this value is much smaller than the calorimetric unfolding enthalpy. Even though the two-state model allows a perfect simulation of the CD unfolding transition, the combination of CD spectroscopy and two-state model does not deliver a correct thermodynamic analysis.

A perfect fit of the CD unfolding transition is also obtained with the Zimm−Bragg theory (Figure 8B, dashed green line) using $\sigma = 8 \times 10^{-4}$, $h = -1.1$ kcal/mol, and $N = 123$. This suggests an enthalpy change of 123 × 1.1 = 135.3 kcal/mol, in agreement with the calorimetric result. The nucleation factor $\sigma = 8 \times 10^{-4}$ is considerably larger than $\sigma = 3 \times 10^{-4}$ as derived from the DSC transition, suggesting a reduced cooperativity. This is illustrated by the red solid line in Figure 8B, which was calculated with the same Zimm−Bragg parameters as used to fit the DSC experiment. The predicted transition is considerably sharper (higher cooperativity) than the CD transition and occurs at a 5 °C lower temperature. The DSC transition cannot be used to predict the CD unfolding transition.

The temperature difference between the DSC and CD transitions was observed in all our Apo A-1 measurements (compare Table 1 with Table 2). Apparently, the energetic changes induced by increasing the temperature and recorded by DSC are not immediately carried over into structural changes detected by CD spectroscopy. The CD data suggest that even after thermodynamic destabilization of hydrogen bonds the helical structures of Apo A-1 are loosely retained. An additional temperature increase is necessary to induce the collapse of labile α-helical regions.

Apo A-1 forms oligomers at low temperature with maximum oligomerization at 22 °C.[23] At 45 °C the oligomers are almost completely dissociated, and only monomers are involved in the unfolding process. Oligomer disassociation may however be responsible for the sloping baseline of the initial phase of the CD transition curve leading to an increased width of the transition (lower cooperativity: $\sigma_{CD} > \sigma_{DSC}$). It is known that self-associating apolipoproteins display a concentration-dependent induction of α-helix.[18,19,48] Conversely, disassociation of oligomers would entail a loss in helicity.

The calorimetric criterion for a two-state folding ⇄ unfolding equilibrium is the equivalence of the *measured* calorimetric enthalpy change and the *calculated* conformational

DOI: 10.1021/acs.biochem.5b00238
Biochemistry 2015, 54, 3063−3075

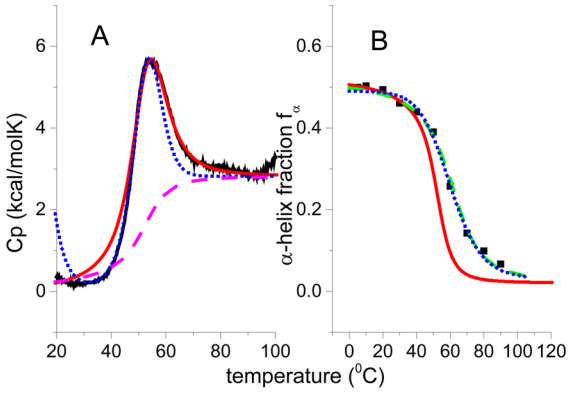

Figure 8. Folding ⇄ unfolding equilibrium of 100 μM Apo A-1 measured with DSC and CD spectroscopy. PBS buffer with 5 mM β-octyl glucoside. (A) DSC experimental data: black line. Zimm–Bragg theory: red solid line, h = −1.1 kcal/mol, σ = 3.0 × 10^{-4}, N = 123, $\Delta C^0_{p,NU}$ = 2.818 kcal/mol·K, T_∞ = 56 °C. Two-state model: blue dotted line, $\Delta H^0_{NU,2\text{-state}}$ = 52.5 kcal/mol, T_0 = 51 °C, $\Delta C^0_{p,NU}$= 2.818 kcal/mol·K. contribution of $\Delta C^0_{p,NU}$ to the unfolding transition: dashed magenta line. (B) CD experimental data: filled squares (■). Two-state model: blue dotted line, T_0 = 60 °C, $\Delta H^0_{NU,2\text{-state}}$ = 31.05 kcal/mol. Zimm–Bragg theory: dashed green line, h = −1.1 kcal/mol, σ = 8 × 10^{-4}, N = 123, T_∞ = 63.5 °C. Zimm–Bragg theory, same parameters as used to fit the DSc experiment in (A): solid red line.

(van't Hoff) enthalpy (see ref 1 and literature cited therein). If the predicted conformational enthalpy deviates from the experimental result, the ratio "predicted enthalpy/measured enthalpy" is defined as cooperativity.[28]

Previous DSC studies of Apo A-1 reported unfolding enthalpies between 50 and 200 kcal/mol with midpoint temperatures in the range of 53–63 °C.[23,26−29,43] The calorimetric criterion was either fulfilled,[26,27] not fulfilled,[28] or a superposition of several two-state processes was suggested.[29,43]

The average values of the present DSC measurements are summarized in Table 1. The calorimetric enthalpy is ΔH^0_{exp} = 123.7 ± 10.6 kcal/mol (T_0 = 52.1 ± 0.6 °C), the Zimm–Bragg theory gives $\Delta H^0_{calc,ZB}$ = 127 ± 7.4 kcal/mol, and the two-state model $\Delta H^0_{calc,2\text{-state}}$ = 112.7 ± 1.8 kcal/mol. The two-state model is characterized by a conformational (van't Hoff) enthalpy $\Delta H^0_{NU,2\text{-state}}$ = 66.7 ± 1.9 kcal/mol.

The *total* heat of unfolding, and not only the conformational enthalpy, must be considered for the molecular interpretation of the folding ⇄ unfolding equilibrium. "It is clear that in considering the energetic characteristics of protein unfolding one has to take into account all energy which is accumulated upon heating and not only the very substantial heat effect associated with gross conformational transitions, that is, all the excess heat effects must be integrated".[38] For example, only the *total* heat of Apo A-1 unfolding divided by the number of unfolded α-helical residues results in the correct hydrogen bond enthalpy h = 1076 ± 79 cal/mol (Table 1), which is consistent with the literature.[5,11]

An increase in heat capacity upon unfolding has been reported for a large number of proteins,[37] and the present result of $\Delta C^0_{p,NU}$ = 2.52 ± 0.09 kcal/mol·K falls in the range expected for a protein with 245 amino acids (see Table 1 of ref 37). An increase in the heat capacity of $\Delta C^0_{p,NU}$ = 2.7 ± 0.9 kcal/mol·K was observed in the very first DSC study of Apo A-1[26,27] but was not reported in later publications.

The Zimm–Bragg theory can be used to calculate the free energy change,ΔG_{NU}, of Apo A-1 unfolding. The unfolding transition takes place between 30 and 70 °C leading to a corresponding change of the growth parameter $s(T)$. The change in free energy for a single amino acid residue, calculated with the parameters of lipid-free Apo A-1 (σ = 9.3 × 10^{-5}, h = −1.1 kcal/mol, N = 115), is then given by

$$g_{NU} = -RT_0 \ln[s(T_2)/(s(T_1)] \quad (12)$$

yielding g_{NU} = 137 cal/mol for the temperature interval defined above. This result is in agreement with g_{NU} = 140 cal/mol obtained for the amphipathic peptide magainin 2 with a completely different method.[45] For two other amphipathic peptides measured under different experimental conditions a value of g_{NU} ≈ 250 cal/mol has been reported.[49,50]

The total free energy of unfolding can thus be calculated as ΔG_{NU} = 115 × 0.137 = 15.8 kcal/mol.

The free energy of unfolding of human Apo A-1 was determined from guanidine HCl denaturation experiments. CD spectra of Apo A-1 were obtained at increasing concentrations of guanidine HCl and evaluated with the two-state model, leading to a free energy of unfolding of ΔG_{NU} = 3.5–4.2 kcal/mol.[42,51] This is significantly smaller than the 15.8 kcal/mol deduced from calorimetric measurements. We therefore used the CD transition curve depicted in Figure 3 to calculate the free energy change with the two-state model according to $\Delta G_{NU} = RT \ln(K_{T_1}/K_{T_2})$.With a conformational enthalpy of ΔH^0_{NU} = 29.6 kcal/mol (deduced from Figure 3), the free energy change caused by temperature-denaturation is found to be ΔG_{NU} = 3.75 kcal/mol (temperature interval of 30–70 °C), in excellent agreement with guanidine HCl denaturation at constant temperature. It thus appears that the low free energy of unfolding is the result of combining the wrong experimental method with the wrong theoretical model for Apo A-1.

Thermodynamic Stabilization of Apo A-1 by Binding to Lipid. The α-helix content of Apo A-1 increased from ∼50% in aqueous solution to ∼75% in excess lipid, consistent with lipid titrations at room temperature.[42] Protein unfolding occurred between 75 and 100 °C, and the midpoint of the transition was shifted to 87.2 ± 2.9 °C involving N = 170 ± 5 amino acid residues. The DSC unfolding transition in the lipid phase is more cooperative with σ = (3.8 ± 1.7) × 10^{-5} than that in the aqueous phase with σ = (9.3 ± 3.3) × 10^{-5}. The total unfolding enthalpy of lipid-bound Apo A-1 was found to be ΔH^0_{exp} = 139.7 ± 13.9 kcal/mol, only moderately larger than the unfolding enthalpy in aqueous solution. As a result, the enthalpy of the hydrogen bond formation in the lipid phase is reduced to h = −792 ± 77 cal/mol. This agrees well with studies of model peptides in hydrophobic solvents which report h = −0.7 to −0.8 kcal/mol (ref 44, Figure 3B). Likewise, α-helix formation of an amphipathic peptide at the membrane surface was characterized by an enthalpy change of h = −0.7 kcal/mol per residue.[45]

Lipid-bound Apo A-1 is stabilized by the formation of 50–60 new α-helical amino acid residues. As deduced above α-helix formation at the bilayer surface is characterized by a change in free energy of g_{NU} = −0.137 kcal/mol per amino acid residue. The total free energy change associated with 55 new α-helical amino acid residues is therefore −7.5 kcal/mol. The enthalpy change caused by the newly formed α-helical amino acid residues is 55 × (−0.8) kcal/mol = −44 kcal/mol. However, lipid binding reduces the hydrogen bond enthalpy of existing

DOI: 10.1021/acs.biochem.5b00238
Biochemistry 2015, 54, 3063–3075

bonds from −1.1 kcal/mol to −0.8 kcal/mol, causing a loss in enthalpy of 120 × 0.3 = 36 kcal/mol. The total enthalpy change is −8.0 kcal/mol, which must be compared to the free energy change −7.7 kcal/mol. The gain in enthalpy is thus the dominant contribution to the free energy and the main driving force for α-helix formation.

Interaction of Apo A-1 with a Nonionic Detergent. Ionic detergents such as SDS *decrease* the helicity of Apo A-1,[52] whereas bilayer-forming lipids *increase* it. In contrast, the α-helix content remains practically *constant* in the nonionic detergent β-octyl glucoside (see Table 3). The midpoint of the unfolding transition is identical or very close to that of the lipid-free Apo A-1, even if the protein is dissolved at micellar concentrations of β-octyl glucoside. The main effect of the addition of detergent is a broadening of the unfolding transition. The calorimetric DSC experiments show a 3-fold increase of the nucleation parameter from $\sigma = 10^{-4}$ in the absence of detergent to $\sigma = 3 \times 10^{-4}$ at $c_{\beta\text{-OG}}$ = 10 mM. This effect is even more pronounced in CD spectroscopy as these measurements can be extended to 37 mM β-octyl glucoside. The CD spectra show a 10-fold increase of the nucleation parameter from $\sigma = 10^{-3}$ in the absence of detergent to $\sigma = 10^{-2}$ at $c_{\beta\text{-OG}}$ = 37 mM. As noted before, the spectroscopic unfolding transitions are distinctly broader than the thermodynamic unfolding transitions and are shifted by 5−8 °C toward higher temperatures.

At $c_{\beta\text{-OG}}$ = 10 mM two separate, reproducible unfolding transitions were observed in DSC experiments (but not in CD measurements), involving 30−40 and 80−90 amino acid residues, respectively. HDX-exchange experiments revealed a long (amino acids 7−115) and a short stretch (amino acids 147−178) of α-helices.[15,17] The shorter α-helix was furthermore adjacent to the unstructured C-terminal domain of the protein. It is thus judicious to assign the low-temperature transition to amino acids 147−178 and the main transition to the longer helix bundle comprising amino acids 7−115.

Two transitions with maxima at 50 and 60 °C have been observed previously.[29] The DSC experiment was run with the protein under reducing conditions as the buffer contained 10 mM dithiothreitol. The unfolding enthalpies were considerably smaller than those reported here, but the enthalpy ratio of pretransition (~25% of total enthalpy) and main transition (~75% of total enthalpy) was similar.

The main effect of β-octyl glucoside is therefore a gradual destabilization of the protein secondary and tertiary structure reflected in a decrease in cooperativity and a stepwise unfolding of separate protein domains.

CONCLUSION

The thermal analysis and molecular interpretation of Apo A-1 unfolding must include the increased heat capacity of the unfolded protein. The corresponding enthalpy accounts for 40−50% of the total unfolding enthalpy.

Excellent curve fittings are achieved with the Zimm−Bragg theory for all DSC and CD folding ⇄ unfolding experiments, both for Apo A-1 in aqueous solution and bound to lipid bilayers. The application of the Zimm−Bragg theory leads to a consistent set of physical parameters. It provides a physical definition of cooperativity in terms of the nucleation factor σ.

The unfolding transitions reported by CD spectroscopy do not coincide with the calorimetric unfolding. The CD transition curves are broader and are shifted by about 5−8 °C toward higher temperatures. CD spectra are therefore not suited for a thermodynamic evaluation of Apo A-1 unfolding.

The conformational (van't Hoff) enthalpies deduced with the two-state model are smaller for CD transition curves than for DSC transitions. The conformational enthalpy accounts for not more than 60% of the total unfolding enthalpy of Apo A-1.

The nonionic detergent β-octyl glucoside destabilizes Apo A-1 without affecting its α-helix content or the unfolding enthalpy. However, the unfolding transition becomes broader and a piecewise unfolding is observed at 10 mM detergent.

Phospholipid stabilizes Apo A-1. The unfolding transition is more cooperative and shifted by 30 °C toward higher temperature. The stability of hydrogen bonds is reduced from $h = -1.1$ kcal/mol in the aqueous phase to $h = -0.8$ kcal/mol in the lipid phase.

It could be argued that it is unclear how well the Zimm−Bragg theory describes the unfolding other proteins. We have therefore analyzed a set of 10 published DSC data of different proteins (including globular proteins) with the two-state model and the Zimm Bragg theory. The average error in reproducing the thermal unfolding transition was 2.7% for the Zimm−Bragg theory and 15% for the two-state model.

AUTHOR INFORMATION

Corresponding Author

*Tel. +41-61-267 2190. Fax: +41-61-267 2189. E-mail: joachim.seelig@unibas.ch.

Funding

Swiss National Science Foundation Grant No. 31003A-129701.

Notes

The authors declare no competing financial interest.

ABBREVIATIONS

CD, circular dichroism; DSC, differential scanning calorimetry; Apo A-1, human apolipoprotein A-1; SUV, small unilamellar vesicle; POPC, 1-palmitoyl-2-oleoyl-*sn*-glycero-3-phosphocholine; POPG, 1-palmitoyl-2-oleoyl-*sn*-glycero-3-phosphoglycerol; PBS, phosphate buffered saline; HDX, amide backbone hydrogen/deuterium exchange

REFERENCES

(1) Zhou, Y., Hall, C. K., and Karplus, M. (1999) The calorimetric criterion for a two-state process revisited. *Protein Sci. 8*, 1064−1074.

(2) Tanaka, A., Kobayashi, D., Senoo, K., and Obata, H. (1999) Possibility for discriminating between two representative non two-state thermal unfolding models of proteins by DSC. *Biosci. Biotechnol. Biochem. 63*, 438−442.

(3) Zimm, B. H., and Bragg, J. K. (1959) Theory of the Phase Transition between Helix and Random Coil in Polypeptide Chains. *J. Chem. Phys. 31*, 526−535.

(4) Zimm, B. H., Doty, P., and Iso, K. (1959) Determination of the parameters for helix formation in poly-gamma-benzyl-L-glutamate. *Proc. Natl. Acad. Sci. U. S. A. 45*, 1601−1607.

(5) Zimm, B. H., and Rice, S. A. (1960) The Helix-Coil Transition in Charged Macromolecules. *Mol. Phys. 3*, 391−407.

(6) Lifson, S., and Roig, A. (1961) Theory of Helix-Coil Transition in Polypeptides. *J. Chem. Phys. 34*, 1963−1974.

(7) Scholtz, J. M., Marqusee, S., Baldwin, R. L., York, E. J., Stewart, J. M., Santoro, M., and Bolen, D. W. (1991) Calorimetric Determination of the Enthalpy Change for the Alpha-Helix to Coil Transition of an Alanine Peptide in Water. *Proc. Natl. Acad. Sci. U. S. A. 88*, 2854−2858.

(8) Scholtz, J. M., Qian, H., York, E. J., Stewart, J. M., and Baldwin, R. L. (1991) Parameters of Helix-Coil Transition Theory for Alanine-Based Peptides of Varying Chain Lengths in Water. *Biopolymers 31*, 1463−1470.

DOI: 10.1021/acs.biochem.5b00238
Biochemistry 2015, 54, 3063−3075

(9) Chou, P. Y., and Scheraga, H. A. (1971) Calorimetric Measurement of Enthalpy Change in Isothermal Helix-Coil Transition of Poly-L-Lysine in Aqueous Solution. *Biopolymers 10*, 657.
(10) Ooi, T., and Oobatake, M. (1991) Prediction of the thermodynamics of protein unfolding: the helix-coil transition of poly(L-alanine). *Proc. Natl. Acad. Sci. U. S. A. 88*, 2859−2863.
(11) Rialdi, G., and Hermans, J. (1966) Calorimetric Heat of Helix-Coil Transition of Poly-L-Glutamic Acid. *J. Am. Chem. Soc. 88*, 5719.
(12) Doig, A. J. (2002) Recent advances in helix-coil theory. *Biophys Chem. 101−102*, 281−293.
(13) Ghosh, K., and Dill, K. A. (2009) Theory for protein folding cooperativity: helix bundles. *J. Am. Chem. Soc. 131*, 2306−2312.
(14) Saito, H., Dhanasekaran, P., Nguyen, D., Deridder, E., Holvoet, P., Lund-Katz, S., and Phillips, M. C. (2004) alpha-Helix formation is required for high affinity binding of human apolipoprotein A-I to lipids. *J. Biol. Chem. 279*, 20974−20981.
(15) Phillips, M. C. (2013) New insights into the determination of HDL structure by apolipoproteins: Thematic review series: high density lipoprotein structure, function, and metabolism. *J. Lipid Res. 54*, 2034−2048.
(16) Mei, X., and Atkinson, D. (2011) Crystal structure of C-terminal truncated apolipoprotein A-I reveals the assembly of high density lipoprotein (HDL) by dimerization. *J. Biol. Chem. 286*, 38570−38582.
(17) Chetty, P. S., Mayne, L., Lund-Katz, S., Stranz, D., Englander, S. W., and Phillips, M. C. (2009) Helical structure and stability in human apolipoprotein A-I by hydrogen exchange and mass spectrometry. *Proc. Natl. Acad. Sci. U. S. A. 106*, 19005−19010.
(18) Stone, W. L., and Reynolds, J. A. (1975) The self-association of the apo-Gln-I and apo-Gln-II polypeptides of human high density serum lipoproteins. *J. Biol. Chem. 250*, 8045−8048.
(19) Gwynne, J., Palumbo, G., Osborne, J. C., Jr., Brewer, H. B., Jr., and Edelhoch, H. (1975) The self-association of apoA-II, an apoprotein of the human high density lipoprotein complex. *Arch. Biochem. Biophys. 170*, 204−212.
(20) Vitello, L. B., and Scanu, A. M. (1976) Studies on human serum high density lipoproteins. Self-association of apolipoprotein A-I in aqueous solutions. *J. Biol. Chem. 251*, 1131−1136.
(21) Formisano, S., Brewer, H. B., Jr., and Osborne, J. C., Jr. (1978) Effect of pressure and ionic strength on the self-association of Apo-A-I from the human high density lipoprotein complex. *J. Biol. Chem. 253*, 354−359.
(22) Yokoyama, S., Tajima, S., and Yamamoto, A. (1982) The process of dissolving apolipoprotein A-I in an aqueous buffer. *J. Biochem 91*, 1267−1272.
(23) Zehender, F., Ziegler, A., Schonfeld, H. J., and Seelig, J. (2012) Thermodynamics of Protein Self-Association and Unfolding. The Case of Apolipoprotein A-I. *Biochemistry 51*, 1269−1280.
(24) Donovan, J. M., Benedek, G. B., and Carey, M. C. (1987) Self-association of human apolipoproteins A-I and A-II and interactions of apolipoprotein A-I with bile salts: quasi-elastic light scattering studies. *Biochemistry 26*, 8116−8125.
(25) Jayaraman, S., Abe-Dohmae, S., Yokoyama, S., and Cavigiolio, G. (2011) Impact of self-association on function of apolipoprotein A-I. *J. Biol. Chem. 286*, 35610−35623.
(26) Tall, A. R., Small, D. M., Shipley, G. G., and Lees, R. S. (1975) Apoprotein stability and lipid-protein interactions in human plasma high density lipoproteins. *Proc. Natl. Acad. Sci. U. S. A. 72*, 4940−4942.
(27) Tall, A. R., Shipley, G. G., and Small, D. M. (1976) Conformational and thermodynamic properties of apo A-1 of human plasma high density lipoproteins. *J. Biol. Chem. 251*, 3749−3755.
(28) Gursky, O., and Atkinson, D. (1996) Thermal unfolding of human high-density apolipoprotein A-1: implications for a lipid-free molten globular state. *Proc. Natl. Acad. Sci. U. S. A. 93*, 2991−2995.
(29) Suurkuusk, M., and Hallen, D. (1999) Denaturation of apolipoprotein A-I and the monomer form of apolipoprotein A-I-Milano. *Eur. J. Biochem. 265*, 346−352.
(30) Suurkuusk, M., and Hallen, D. (1999) Apolipoprotein A-I(Milano) unfolds via an intermediate state as studied by differential scanning calorimetry and circular dichroism. *Eur. J. Biochem. 264*, 183−190.
(31) Reed, J., and Reed, T. A. (1997) A set of constructed type spectra for the practical estimation of peptide secondary structure from circular dichroism. *Anal. Biochem. 254*, 36−40.
(32) Schwarz, G., and Seelig, J. (1968) Kinetic Properties and Electric Field Effect of Helix-Coil Transition of Poly(Gamma-Benzyl L-Glutamate) Determined from Dielectric Relaxation Measurements. *Biopolymers 6*, 1263−&.
(33) Thompson, P. A., Eaton, W. A., and Hofrichter, J. (1997) Laser temperature jump study of the helix reversible arrow coil kinetics of an alanine peptide interpreted with a 'kinetic zipper' model. *Biochemistry 36*, 9200−9210.
(34) Sevugan Chetty, P., Mayne, L., Kan, Z. Y., Lund-Katz, S., Englander, S. W., and Phillips, M. C. (2012) Apolipoprotein A-I helical structure and stability in discoidal high-density lipoprotein (HDL) particles by hydrogen exchange and mass spectrometry. *Proc. Natl. Acad. Sci. U. S. A. 109*, 11687−11692.
(35) Davidson, N. (1962) *Statistical Mechanics*, p 385, McGraw-Hill, New York.
(36) Yang, A. S., and Honig, B. (1995) Free energy determinants of secondary structure formation: I. alpha-Helices. *J. Mol. Biol. 252*, 351−365.
(37) Myers, J. K., Pace, C. N., and Scholtz, J. M. (1995) Denaturant m values and heat capacity changes: relation to changes in accessible surface areas of protein unfolding. *Protein Sci. 4*, 2138−2148.
(38) Privalov, P. L., and Dragan, A. I. (2007) Microcalorimetry of biological macromolecules. *Biophys Chem. 126*, 16−24.
(39) Lagerstedt, J. O., Budamagunta, M. S., Liu, G. S., DeValle, N. C., Voss, J. C., and Oda, M. N. (2012) The "beta-clasp" model of apolipoprotein A-I–a lipid-free solution structure determined by electron paramagnetic resonance spectroscopy. *Biochim. Biophys. Acta 1821*, 448−455.
(40) Lagerstedt, J. O., Budamagunta, M. S., Oda, M. N., and Voss, J. C. (2007) Electron paramagnetic resonance spectroscopy of site-directed spin labels reveals the structural heterogeneity in the N-terminal domain of apoA-I in solution. *J. Biol. Chem. 282*, 9143−9149.
(41) Saito, H., Dhanasekaran, P., Nguyen, D., Holvoet, P., Lund-Katz, S., and Phillips, M. C. (2003) Domain structure and lipid interaction in human apolipoproteins A-I and E, a general model. *J. Biol. Chem. 278*, 23227−23232.
(42) Tanaka, M., Koyama, M., Dhanasekaran, P., Nguyen, D., Nickel, M., Lund-Katz, S., Saito, H., and Phillips, M. C. (2008) Influence of tertiary structure domain properties on the functionality of apolipoprotein A-I. *Biochemistry 47*, 2172−2180.
(43) Brouillette, C. G., Dong, W. J., Yang, Z. W., Ray, M. J., Protasevich, II, Cheung, H. C., and Engler, J. A. (2005) Forster resonance energy transfer measurements are consistent with a helical bundle model for lipid-free apolipoprotein A-I. *Biochemistry 44*, 16413−16425.
(44) Luo, P., and Baldwin, R. L. (1997) Mechanism of helix induction by trifluoroethanol: a framework for extrapolating the helix-forming properties of peptides from trifluoroethanol/water mixtures back to water. *Biochemistry 36*, 8413−8421.
(45) Wieprecht, T., Apostolov, O., Beyermann, M., and Seelig, J. (1999) Thermodynamics of the alpha-helix-coil transition of amphipathic peptides in a membrane environment: implications for the peptide-membrane binding equilibrium. *J. Mol. Biol. 294*, 785−794.
(46) Paula, S., Sus, W., Tuchtenhagen, J., and Blume, A. (1995) Thermodynamics of Micelle Formation as a Function of Temperature - a High-Sensitivity Titration Calorimetry Study. *J. Phys. Chem. 99*, 11742−11751.
(47) Majhi, P. R., and Blume, A. (2001) Thermodynamic characterization of temperature-induced micellization and demicellization of detergents studied by differential scanning calorimetry. *Langmuir 17*, 3844−3851.
(48) Yokoyama, S., Kawai, Y., Tajima, S., and Yamamoto, A. (1985) Behavior of human apolipoprotein E in aqueous solutions and at interfaces. *J. Biol. Chem. 260*, 16375−16382.

DOI: 10.1021/acs.biochem.5b00238
Biochemistry 2015, 54, 3063−3075

(49) Li, Y., Han, X., and Tamm, L. K. (2003) Thermodynamics of fusion peptide-membrane interactions. *Biochemistry 42*, 7245−7251.
(50) Fernandez-Vidall, M., Jayasinghe, S., Ladokhin, A. S., and White, S. H. (2007) Folding amphipathic helices into membranes: Amphiphilicity trumps hydrophobicity. *J. Mol. Biol. 370*, 459−470.
(51) Edelstein, C., and Scanu, A. M. (1980) Effect of guanidine hydrochloride on the hydrodynamic and thermodynamic properties of human apolipoprotein A-I in solution. *J. Biol. Chem. 255*, 5747−5754.
(52) Makino, S., Tanford, C., and Reynolds, J. A. (1974) The interaction of polypeptide components of human high density serum lipoprotein with detergents. *J. Biol. Chem. 249*, 7379−7382.

DOI: 10.1021/acs.biochem.5b00238
Biochemistry 2015, 54, 3063−3075